ELSEVIER

Atherosclerosis 136 (1998) 203–216

ATHEROSCLEROSIS

A specific 15-lipoxygenase inhibitor limits the progression and monocyte–macrophage enrichment of hypercholesterolemia-induced atherosclerosis in the rabbit

Thomas M.A. Bocan [a,*], Wendy S. Rosebury [a], Sandra Bak Mueller [a], Susan Kuchera [a], Kathryn Welch [a], Alan Daugherty [b], Joseph A. Cornicelli [a]

[a] *Department of Vascular and Cardiac Diseases, Parke–Davis Pharmaceutical Research, Division of Warner Lambert Company, 2800 Plymouth Road, Ann Arbor, MI 48105, USA*

[b] *Cardiovascular Division, Department of Medicine and Department of Biochemistry and Molecular Biophysics, Washington University School of Medicine, St. Louis, MO 63110, USA*

Received 25 March 1997; received in revised form 28 July 1997; accepted 18 August 1997

Abstract

Oxidant signalling and lipoprotein oxidation may play important roles in atherosclerotic lesion development. Given coincident localization of 15-lipoxygenase (15-LO), stereospecific products of 15-LO and epitopes of modified LDL in atherosclerotic lesions, we hypothesized that inhibition of 15-LO by PD146176, an inhibitor of 15-LO with an IC_{50} in cells or isolated enzyme of 0.5–0.8 μM, may limit atherosclerotic lesion development through regulation of monocyte–macrophage enrichment. Rabbits exposed to chronic endothelial denudation of the iliac-femoral artery were meal-fed a 0.25% cholesterol (C), 3% peanut oil (PNO), 3% coconut oil (CNO) diet twice daily with and without 175 mg/kg PD146176 for 12 weeks. In a second study, atherosclerotic lesions were pre-established in rabbits through chronic endothelial denudation and meal-fed a 0.5% C, 3% PNO, 3% CNO diet for 9 weeks and a 0% C/fat diet for 6 weeks prior to an 8 week administration of PD146176 at 175 mg/kg, q.d. Plasma total and lipoprotein cholesterol exposure were similar in control and PD146176-treated animals in both studies but PD146176 increased plasma triglyceride exposure 2- to 4-fold. Plasma PD146176 concentrations ranged from 99 to 214 ng/ml at 2 h post-dose. In the progression study, the iliac-femoral monocyte–macrophage area was reduced 71%, cross-sectional lesion area was unchanged and cholesteryl ester (CE) content was reduced 63%. In the regression study, size and macrophage content of iliac-femoral, fibrous plaque-like lesions were decreased 34%, CE content was reduced 19% and gross extent of thoracic aortic lesions were reduced 41%. We conclude that PD146176 can limit monocyte–macrophage enrichment of atherosclerotic lesions and can attenuate development of fibrofoamy and fibrous plaque lesions in the absence of changes in plasma total or lipoprotein cholesterol concentrations. © 1998 Warner Lambert Company. Published by Elsevier Science Ireland Ltd.

Keywords: 15-lipoxygenase; Atherosclerosis; Macrophages; Oxidant signalling

1. Introduction

Oxidative modification of plasma lipoproteins within the vessel wall is presumably an extracellular event which has been implicated in the progression of atherosclerosis [1]. The concept that plasma lipoproteins infiltrate the arterial wall at sites of endothelial injury/dysfunction, decorate extracellular matrix and become modified is not new [2,3] but mechanisms responsible for generation of the modifying agent are emerging. Based on observations that oxidized lipoproteins were involved in regulation of chemokines [4], adhesion molecule [5] and that general antioxidant agents such as probucol [6–11], vitamins E and C [11,12] and butylated hydroxytoluene (BHT) [13] were

* Corresponding author. Tel.: +1 313 9967383; fax: +1 313 9963135; e-mail: bocant@aa.wl.com

0021-9150/98/$19.00
PII S0021-9150(97)00204-9

effective at limiting atherosclerotic lesion progression, oxidant signalling appears to play an integral role in atherosclerotic lesion development. A new enzyme specific target, arachidonate 15-lipoxygenase (15-LO), has emerged as being involved in lipoprotein oxidation [14] and the enzyme products may be important in regulation of proatherogenic molecules. Arachidonate 15-lipoxygenase is a lipid-peroxidizing enzyme which is present in atherosclerotic lesions. Investigators have found stereospecific hydroxy fatty acids that can be ascribed to 15-LO activity in extracts of vascular atherosclerotic tissue from animals [15] and humans [16]. Hiltunen et al. have observed 15-LO protein and mRNA in early stages of atherosclerosis in animals [17], while others have colocalized 15-LO mRNA with epitopes of modified LDL and macrophage-rich areas of rabbit and human lesions [14,18]. In vitro studies have shown that non-specific inhibitors of lipoxygenase such as ETYA, piriprost and A64077 can ablate macrophage-mediated oxidation of LDL in vitro [19]. In addition, we have shown that inhibition of 15-LO with PD146176, a specific inhibitor of 15-LO lacking antioxidant properties, can attenuate the development of dietary cholesterol-induced atherosclerotic lesions in the rabbit [20]. In contrast to our previous investigation [20], the current study addresses whether 15-LO inhibition specifically alters the accumulation of monocyte–macrophages within atherosclerotic lesions. In addition, this study assesses whether the 15-LO inhibitor, PD146176, can alter the progression or induce regression of preestablished atherosclerotic lesions.

Oxidized LDL, lipid hydroperoxides and other products of lipid oxidation have been shown to be effective modulators of many gene products that may be considered proatherogenic. These include vascular cell adhesion molecule-1 (VCAM-1) [21] and colony stimulating factors [4]. VCAM-1 expression has been shown to be regulated by TNF-α, PDGF, TGF-β [22], IL-4, lipopolysaccharide (LPS), IFN-γ [23] and lysophosphatidylcholine (lyso-PC) [5], a product of phospholipid oxidation. Transient overexpression of 15-LO in endothelial cells has been shown to augment TNF induced VCAM-1 expression [24]. Minimally oxidized LDL has been noted to induce the expression of MCP-1, a potent chemotactic factor for monocytes [25]. Since the expression of adhesion molecules and monocyte chemotactic factors can be modulated by products of lipid oxidation which may be produced by the action of 15-LO, we hypothesized that inhibition of 15-LO would limit the development of atherosclerosis by specifically regulating the monocyte–macrophage enrichment of the artery.

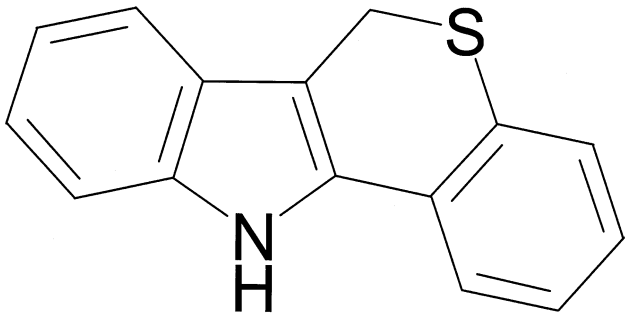

Fig. 1. Chemical structure of PD146176

2. Methods

2.1. Experimental design

Two separate studies were performed. In a study designed to assess the effect of PD146176 on the initiation and progression of atherosclerosis, termed the progression study, male New Zealand White rabbits (Kuiper Farms, Gary, IN) weighing 1.2–1.5 kg were meal-fed 40 g of a diet (Purina 5321) supplemented with 0.25% C, 3% PNO, and 3% CNO with and without 175 mg/kg PD146176 at approximately 07:00 h and 15:00 h daily for a total of 12 weeks. PD146176 is a specific 15-LO inhibitor which has been shown to lack antioxidant properties and to have no or minimal inhibitory activity against 5- and 12-lipoxygenase and cyclooxygenase I and II [20] and is depicted in Fig. 1. The compound was synthesized as previously described [26]. Coincident with diet initiation, a chronic endothelial injury was induced in the iliac-femoral artery by surgically inserting a sterile nylon monofilament through the medial saphenous artery of the right leg to the level of the diaphragm. The monofilament was secured and maintained in place for the entire 12 weeks of the study. Surgical procedures were performed on animals anesthetized with 10 mg/kg xylazine (MILES, Shawnee Mission, KS) and 33 mg/kg ketamine HCl (Fort Dodge Laboratories, Fort Dodge, IA) in accordance with a vertebrate use form approved by the Parke–Davis institutional review board. The animals were randomized based on animal number into equal groups of eight animals prior to surgery. The progression control was maintained on the cholesterol plus fat diet for the duration of the study and eight additional animals were administered 175 mg/kg PD146176, b.i.d., in the cholesterol/fat diet.

A second study designed to assess the effect of PD146176 on pre-established atherosclerotic lesions, termed the regression study, was performed. Male New Zealand White rabbits (Kuiper Farms, Gary, IN) weighing 1.2–1.5 kg were meal-fed a diet (Purina 5321) supplemented with 0.5% C, 3% PNO, and 3% CNO

diet for a total of 9 weeks and a 0% C, 3% PNO, and 3% CNO diet (fat diet) for 6 weeks to induce atherosclerotic lesions prior to an 8 week administration of PD146176 or chow/fat diet. The dietary regimen consisted of feeding 40 g for the first week, 50 g for 4 weeks, 60 g for 4 weeks, 70 g for the next 6 weeks, and 80 g for the final 8 weeks. After 1 week of diet initiation, a chronic endothelial injury was induced in the iliac-femoral artery as described above. After the initial 15-week lesion induction phase, the animals were randomized on the basis of their 24 h post-meal plasma total cholesterol concentrations into three statistically similar groups of eight animals each. A time zero group was necropsied at 15 weeks prior to drug administration while a progression control group was maintained on the fat diet for the remaining 8 weeks of the study. PD146176 was administered at 175 mg/kg q.d. as a diet admixture in the fat containing diet for the final 8 weeks. All diets were freshly prepared on a monthly basis.

2.2. Biochemical methods

The inhibition of rabbit reticulocyte 15-LO was assessed as previously described [20]. Briefly, a solution of PD146176 and substrate were added to a known amount of purified enzyme and incubated at 4°C for 10 min. The reaction was stopped by addition of methanol and the samples were reduced with triphenylphosphine (100 μg) before being subjected to reverse phase (r.p.) HPLC for quantification of 13-HODE. Studies in intact cells were performed using IC21 mouse macrophages which were stably transfected with human 15-LO. The transfected cells were plated at 20 000 cells per 35 mm tissue culture plate and placed in the incubator overnight. The media was removed and the cultures were rinsed once with PBS. Cultures were then incubated in 1 ml of PBS containing 100 μM linoleic acid in the presence or absence of varying concentrations of PD146176 for 30 min at 37°C. The PBS was extracted, reduced and 13-HODE was quantified by r.p. HPLC. Studies designed to assess the reversibility of enzyme inhibition by PD146176 were also performed. Transfected IC21 cells seeded at 20 000 cells per 35 mm tissue culture plate were cultured overnight. PD146176 was added in complete culture media at a concentration of 10 μM to two sets of cells and allowed to incubate for an additional 24 h. The media containing the drug was removed, the cells were rinsed briefly with PBS and 1 ml of PBS containing 100 μM linoleic acid was added to one set of cells and incubated for 30 min at 37°C. The second set of cells were washed with PBS and then fresh complete culture media without drug was added. After a 40 min incubation at 37°C in complete culture media, the media was removed, the cells were washed briefly in PBS and 1 ml of PBS containing 100 μM linoleic acid was added to one set of cells and incubated for 30 min at 37°C. In the latter two experiments the media was extracted and 13-HODE was quantified as noted above.

Plasma cholesterol and triglyceride concentrations were determined enzymatically throughout the study on an Abbott VP Series II Bichromatic Analyzer (Abbott, Chicago, IL) [27,28] using the Boehringer–Mannheim total cholesterol reagent (Indianapolis, IN) and the Abbott triglyceride reagent. Lipid measurements were performed monthly or biweekly on plasma samples collected 24 h post-meal. Plasma lipoprotein cholesterol distribution was measured by a high performance gel filtration chromatography method [29].

Plasma concentrations of PD146176 were determined by HPLC. Blood was collected 2 h post-morning dose and plasma from control and treated animals was incubated with NaOH. The plasma was extracted with pentane:methyl *t*-butyl ether (3:2) after addition of a known amount of a structural analog of PD146176 which served as an internal standard. The organic layer was recovered, dried under nitrogen, reconstituted with methanol:water (4:1) and PD146176 was chromatographed on a 250 mm Zorbax SB-C18 column, eluted with acetonitrile in 25 mM ammonium phosphate and quantified by ultraviolet absorbance.

A 3 cm segment of the iliac-femoral artery adjacent to that collected for histologic evaluation and the entire descending thoracic aorta were assayed for total cholesterol, cholesteryl ester (CE), free cholesterol (FC), and total phospholipid (PL) content. The lipids were extracted into chloroform:methanol (2:1) by the procedure of Folch et al. [30] and 300–500 μl of an internal standard, i.e. 200 mg/ml solution of 4-hydroxy-cholesterol in ethylacetate:acetone (2:1), was added to the extracts of the iliac-femoral and thoracic aortic samples. After extraction, the organic phase was dried under nitrogen and redissolved in iso-octane/tetrahydrofuran (97:3). The lipid content and composition of the vessels were measured using an HPLC method [31]

2.3. Cytochemical methods

For histologic evaluation of lesions in the iliac-femoral and aortic arch regions, the first 1 cm segment of the iliac-femoral artery distal to the aortic-iliac bifurcation and ascending aorta distal to the aortic valves, respectively, were fixed in 10% neutral buffered formalin for <24 h. The vessels were dehydrated, cleared in xylene, and infiltrated with molten paraffin (<60°C) using a Tissue Tek VIP autoprocessor (Miles Scientific, Elkhart, IN). The tissue segments were embedded in paraffin and sectioned at 5 μm with a Reichert–Jung microtome (Baxter, McGaw Park, IL). In order to obtain a thorough representation of the histologic appearance of the iliac-femoral lesion, three ribbons of 20

sections each were cut at approximately 100 μm intervals. Three pairs of sections, i.e. one pair from each ribbon, were affixed to ProbeOn Plus™ (Fisher Scientific, Cincinnati, OH) glass slides overnight on a warming plate maintained at <45°C and stored until stained. The general histologic character and nature of the extracellular matrix were evaluated in hematoxylin and eosin and Verhoeff's elastica stained sections [32]. The cellular composition of lesions was determined using antibodies to monocyte–macrophages (RAM11, DAKO, Carpinteria, CA) [33] and smooth muscle cells (SMC; HHF35, ENZO Diagnostics, NY) [34]. The presence and localization of 15-lipoxygenase were evaluated using a purified IgG fraction of a polyclonal sheep anti-rabbit reticulocyte 15-lipoxygenase antibody. The immunohistochemical staining of monocyte–macrophages, SMC and 15-lipoxygenase were performed as described previously [35] except that a biotinylated rabbit anti-sheep IgG antibody was used in the identification of 15-lipoxygenase antigen and 3-amino-9-ethylcarbazole (AEC) was used as the peroxidase substrate. As a test for nonspecific staining, the primary antibody was replaced with normal non-immune serum from the same species in which the primary antibody was made. It was determined that non-specific immunostaining was absent. Colocalization of 15-lipoxygenase staining and RAM11(+) monocyte–macrophages and/or actin(+) SMC was also performed as noted above [35] with several exceptions. Between each immunohistochemical procedure, i.e. 15-LO, RAM11(+) macrophages or actin(+) SMC, the sections were incubated overnight at 4°C in 0.2 M glycine hydrochloride, pH 2.4, to displace the primary antibody while leaving the precipitating chromogenic substrate. In addition to peroxidase, alkaline phosphatase conjugated avidin–biotin complexes and various precipitating chromogenic substrates were used.

2.4. Morphometric methods

Sections of the iliac-femoral artery and aortic arch were stained using Verhoeff's elastica stain or with immunochemical markers for monocyte–macrophages. The stained sections were subsequently used for quantification of lesion, vessel and medial size or extent of monocyte–macrophage involvement within the lesion. Gross extent of atherosclerosis within the thoracic aorta was also measured. Morphometric analyses of the iliac-femoral artery and aortic arch were performed on a Power Macintosh 8100/80 AV computer using the public domain NIH Image program (written by Wayne Rasband at the US National Institutes of Health and available from the Internet by anonymous ftp from zippy.nimh.nih.gov or on floppy disk from NTIS, 5285 Port Royal Road, Springfield, VA 22161, Part PB93-504868). Digital images calibrated for magnification of two different Verhoeff's elastica stained sections were collected using a Dage-MTI CCD72 camera (Michigan City, IN) attached to a Leitz Diaplan microscope at a magnification of 2.529 $\times$ to 429 $\times$ (Nushbaum, Cincinnati, OH). Brightness and contrast of the illuminated section were optimized to maximize grey level intensities. Binary images were generated, the external elastic lamina (EEL), internal elastic lamina (IEL) and lumen were identified. Lumen area and areas circumscribed by the IEL and EEL were filled with a uniform grey level and quantified. Lesion area was defined as the difference between the IEL and lumen area while medial area equalled the EEL area minus the IEL area.

Monocyte–macrophage area identified as RAM11-positive regions in sections adjacent to those used in the determination of lesion and vessel size was also examined using image analysis techniques. Digital images calibrated for magnification of two sections stained with RAM11 were collected as noted above to maximize identification of the brown-black immunoprecipitate. Binary images were generated and using inflection points in the grey level histogram as an objective indicator of the RAM11-positive material the area of monocyte–macrophages was determined.

Iliac-femoral and aortic arch lesion and macrophage areas were determined for each specimen and the mean per group was calculated based on the mean specimen area. The percent lesion coverage of the thoracic aorta was also determined in the lesion regression study.

2.5. Statistical analyses

All statistical comparisons of the biochemical and morphometric data were made relative to the untreated hypercholesterolemic progression and time zero control. Total plasma and lipoprotein cholesterol exposures of the animals during the drug treatment phase were determined by applying the trapezoidal rule [36] to the cholesterol time curves from time zero to necropsy. An analysis of variance procedure followed by a least significant difference test or one-tailed Student's t-test for comparisons made relative to the untreated controls were used [37]. All data were collected in a double-blinded fashion and specimens were ascribed to their respective treatment group after the biochemical and morphometric measurements were obtained. All data are represented as mean $\pm$ S.E.M.

3. Results

3.1. Kinetics of 15-LO inhibition by PD146176

PD146176 dose-dependently inhibited purified rabbit reticulocyte 15-LO with an IC_{50} of 0.54 ± 0.02 μM (Mean $\pm$ S.E.M.) (Fig. 2). In intact IC21 cells trans-

Table 1
Plasma lipid and lipoprotein levels

Treatment	Plasma total cholesterol (mg/dl)	Plasma VLDL cholesterol (mg/dl)	Plasma LDL cholesterol (mg/dl)	Plasma triglyceride (mg/dl)	Plasma total cholesterol exposure (mg·day/dl)	Plasma VLDL-C exposure (mg·day/dl)	Plasma LDL-C exposure (mg·day/dl)	Plasma triglyceride exposure (mg·day/dl)
Lesion progression study								
Progression control	878 ± 114	531 ± 94	295 ± 25	83 ± 5	68615 ± 8239	31318 ± 5179	32357 ± 3432	7265 ± 504
PD146176 (175 mg/kg, b.i.d.)	469 ± 104*	179 ± 48*	265 ± 68	561 ± 160*	55826 ± 9428	24165 ± 6291	30083 ± 4130	29918 ± 5399*
Lesion regression study								
Progression control	267 ± 76	49 ± 17	175 ± 60	43 ± 4	23408 ± 4467	5304 ± 1914	15709 ± 3205	3804 ± 362
PD146176 (175 mg/kg, q.d.)	259 ± 57	62 ± 23	159 ± 40	38 ± 6	35722 ± 9542	7869 ± 1494	16072 ± 1380	9978 ± 2589

Data are expressed as mean ± S.E.M.
Total and lipoprotein cholesterol exposure are determined as the area under the cholesterol-time curve during the treatment phase of each experiment.
* Denotes statistically significant difference from respective progression control at $P < 0.05$.

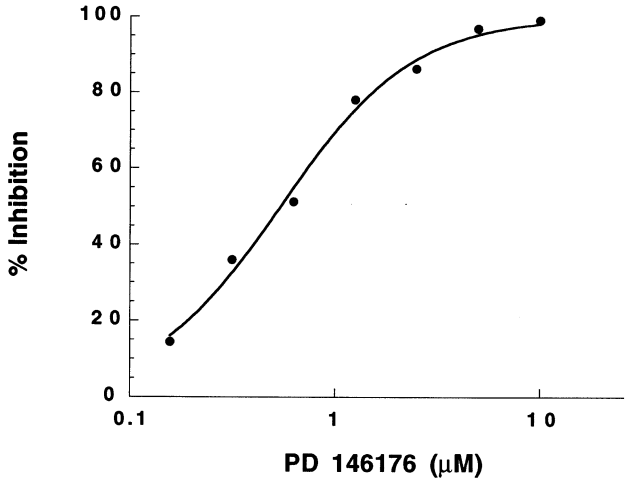

Fig. 2. Titration curve of varying PD146176 concentrations against purified rabbit reticulocyte 15-LO

fected with human 15-LO, PD146176 inhibited 13-HODE production with an IC_{50} of 0.81 ± 0.19 μM. Incubation of the transfected IC-21 cells with 10 μM PD146176 overnight inhibited the generation of 13-HODE by 93% irrespective of whether the subsequent 30 min incubation with linoleic acid was performed in the presence or absence of 10 μM PD146176. However, if the cells were washed and cultured in fresh media for 40 min prior to the 30 min incubation with linoleic acid the generation of 13-HODE was only marginally inhibited, i.e. 18%.

3.2. Plasma and organ measurements

3.2.1. Lesion progression study

Over the first 6 weeks of the study, plasma total cholesterol concentrations increased $\sim$15-fold and remained relatively constant during the subsequent 8 weeks in untreated animals (Fig. 3A). Plasma total cholesterol concentrations in the PD146176 treated animals were comparable to controls over the first 8 weeks; however, at necropsy plasma total cholesterol concentrations were reduced 47%. Associated with the reduction in plasma total cholesterol concentration was a 66% decrease in very low density lipoprotein-cholesterol concentration (VLDL-C) (Table 1). Although mean plasma total and lipoprotein cholesterol concentrations were reduced, plasma total cholesterol, VLDL-C and low density lipoprotein-cholesterol (LDL-C) exposure were unchanged (Table 1). Plasma triglyceride levels remained relatively constant in the control animals, i.e. 56–87 mg/dl; however, in the PD146176 treated animals plasma triglycerides doubled within 1 week of treatment and by the end of the study were increased 6-fold (Fig. 3B) which resulted in a 4-fold increase in plasma triglyceride exposure (Table 1). No differences in body weights and blood hematocrits were noted in the two groups.

Plasma PD146176 concentrations were 45.7 ± 11.6 ng/ml at 2 h post-dose after 1 week and 213.6 ± 122.5 ng/ml after 12 weeks of treatment.

Vessel cholesterol content were reduced. Iliac-femoral and thoracic aortic cholesteryl ester content were reduced 63 and 51% (Table 2), respectively, while the relative lipid weight percentages were comparable, i.e. 39–54% CE, 24–28% FC, 22–36% PL.

3.2.2. Lesion regression study

During the hypercholesterolemic phase, i.e. first 9 weeks of the study, plasma total cholesterol concentrations rose to $\sim$2200 mg/dl but decreased to 700 mg/dl during the subsequent 6 week plasma cholesterol normalization phase (Fig. 4A). Lipoprotein cholesterol concentrations mirrored the changes in plasma total cholesterol (Fig. 4B, C). PD146176 administration following the plasma cholesterol normalization phase had no effect on mean concentration of plasma total cholesterol, VLDL-C, LDL-C or plasma total and lipoprotein cholesterol exposure (Table 1). As in the lesion progres-

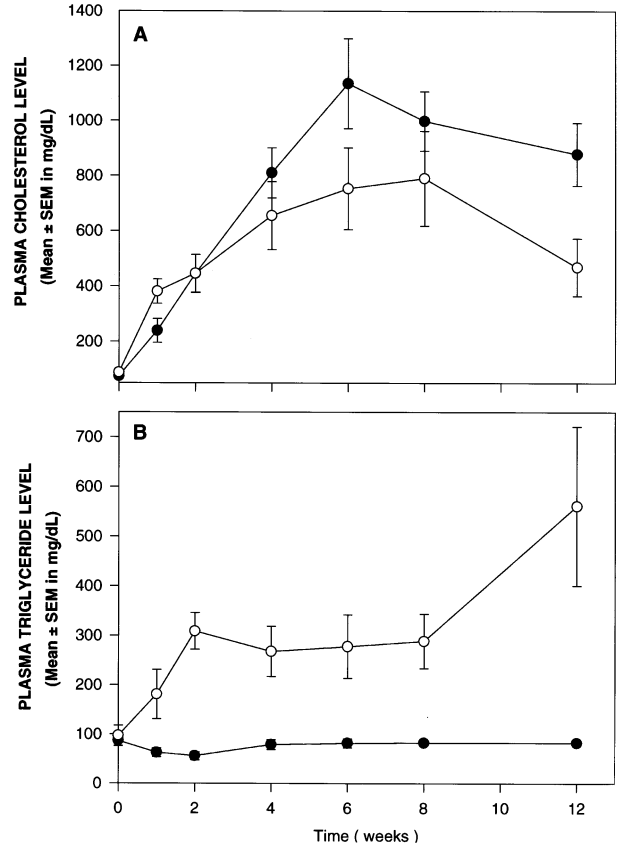

Fig. 3. Line plot of plasma total cholesterol (Panel A) and triglyceride concentrations (Panel B) over the course of the lesion progression study. Data are expressed as mean $\pm$ S.E.M. in mg/dl after treatment with 175 mg/kg PD146176, b.i.d. Plasma total cholesterol concentrations at 12 weeks and plasma triglyceride levels throughout the study were significantly different from the progression control at $P < 0.05$. Progression control, ●; PD146176 (175 mg/kg, b.i.d.), ○.

Table 2
Thoracic aorta and iliac-femoral artery lipid content and distribution

Treatment	Thoracic aorta (μg/mg dry defatted tissue weight)			Iliac-femoral artery (μg/mg dry defatted tissue weight)		
	Cholesteryl ester	Free cholesterol	Total phospholipids	Cholesteryl ester	Free cholesterol	Total phospholipids
Lesion progression study						
Progression control	30.7 ± 7.2	14.5 ± 2.8	14.5 ± 0.6	67.3 ± 15.2	29.7 ± 5.6	27.5 ± 9.3
PD146176 (175 mg/kg, b.i.d.)	15.0 ± 9.2	9.5 ± 3.5	14.0 ± 1.7	24.6 ± 7.2*	13.9 ± 3.3*	11.4 ± 1.3*
Lesion regression study						
Time zero control	204.7 ± 49.9	87.2 ± 23.0	26.6 ± 3.4	257.0 ± 42.4	62.3 ± 5.9	39.9 ± 9.2
Progression control	283.3 ± 71.3	143.0 ± 32.9	46.0 ± 7.4	220.8 ± 25.9	71.7 ± 11.5	39.0 ± 2.8
PD146176 (175 mg/kg, q.d.)	181.3 ± 38.7***	91.7 ± 21.4***	50.1 ± 13.0**	178.9 ± 23.9**	63.7 ± 11.1	33.0 ± 2.9***

Data are expressed as mean ± S.E.M.
* Denotes statistically significant difference from respective progression control at $P<0.05$.
** Denotes statistically significant difference from time zero control at $P<0.10$.
*** Denotes statistically significant difference from respective progression control at $P<0.10$.

sion study, plasma triglyceride levels and exposure increased 2- to 3-fold with PD146176 treatment (Table 1).

Plasma PD146176 concentrations were 99.4 ± 31.0 ng/ml at 2 h post-dose after 7 weeks of treatment.

Iliac-femoral and thoracic aortic cholesteryl ester content were reduced 19 and 36% by PD146176 (Table 2), respectively, while the relative lipid weight percentages were comparable among all groups, i.e. 56–72% CE, 17–30% FC, 9–16% PL.

3.3. Histologic and morphometric measurements

3.3.1. Lesion progression study

Iliac-femoral artery and aortic arch atherosclerotic lesions were of several distinct morphologic appearances. In the iliac-femoral artery, the lesions were macrophage- and SMC-enriched; however, the relative distribution and apparent quantity of these cell types varied. In the control group, 67% of the animals had fibrofoamy lesions in the iliac-femoral artery while in the PD146176 treated group 63% of the animals had fibromuscular lesions and 37% had fibrofoamy lesions. Fibromuscular lesions contained predominantly spindle-shaped and actin(+) smooth muscle cells (SMC) and eosinophilic extracellular matrix (Fig. 5A, B). Fibrofoamy lesions were characterized as containing RAM-11(+) monocyte–macrophages, spindle-shaped and actin(+) smooth muscle cells (SMC) and eosinophilic extracellular matrix (Fig. 5C, D). In addition to reducing the incidence of fibrofoamy lesions, PD146176 appeared to qualitatively reduce the amount of monocyte–macrophages within the iliac-femoral lesion (Fig. 6A, B). In the aortic arch, the lesions were primarily fibrofoamy in nature. However, aortic arch lesions were rather infrequent in both control and PD146176-treated animals which precluded morphometric evaluation.

Morphometric evaluation of the diet- and chronic injury-induced iliac-femoral lesions revealed that the cross-sectional lesion area of control and PD146176-treated animals was comparable (Fig. 7). However, PD146176 reduced the monocyte–macrophage, RAM11(+) cell area by 71%. The intimal/medial ratio was similar in both groups, i.e. 0.9–1.0.

3.3.2. Lesion regression study

Histologic evaluation of the iliac-femoral artery and aortic arch not only revealed the presence of fibrofoamy lesions but also fibrous plaque-like lesions in the progression control and PD146176-treated animals. The fibrous plaque was differentiated from the fibrofoamy lesion by the presence of intimal necrosis and cholesterol clefts in addition to RAM11(+) monocyte–macrophages, spindle-shaped and actin(+) SMC, and eosinophilic extracellular matrix (Fig. 5E, F). In the iliac-femoral artery, 87% of the animals had fibrofoamy lesions prior to drug intervention, i.e. time zero control, while 17% of the animals had fibrofoamy lesions and 50% had fibrous plaque lesions in the progression control. The incidence of fibrous plaque lesions in the PD146176-treated animals was comparable to the progression control, i.e. 57%. In the aortic arch, fibrofoamy lesions predominated in both the time zero and progression control animals, i.e. 86–100%. With PD146176 treatment, 57% of the animals had fibroamy lesions and 43% had fibrous plaques in the aortic arch.

Morphometric analysis of the iliac-femoral artery, aortic arch and thoracic aorta was performed and differences among the groups and vascular region were noted. Iliac-femoral lesion size and composition of the PD146176-treated animals were similar to the time zero control. However, PD146176 reduced the iliac-femoral cross-sectional lesion and monocyte–macrophage area by 34% relative to the progression control (Fig. 8A). In

the aortic arch, no difference in lesion size or composition between the progression control and PD146176-treated animals was noted (Fig. 8B). Relative to the time zero control, aortic arch lesion area and monocyte–macrophage content of the progression control and PD146176-treated animals approximately doubled (Fig. 8B). Despite the observation that the aortic arch cross-sectional area and macrophage content were unaffected by PD146176, the extent of fatty streak-like atherosclerotic lesions within the thoracic aorta, i.e. percent of thoracic aorta covered by atherosclerotic lesions, were reduced from 37% lesion coverage in the progression control to 22% coverage in the PD146176-treated animals.

3.4. Immunohistochemial localization of 15-lipoxygenase

Irrespective of vascular region, lesion type, i.e. fibrofoamy lesion (Fig. 5C) or fibrous plaque (Fig. 5E), or experimental protocol, immunohistochemically detectable 15-lipoxygenase staining was observed. Focal areas of 15-LO(+) vascular endothelial cells were noted in 31% of the animals (Fig. 9A). In the iliac-femoral artery, 15-LO staining was associated with endothelial cells adjacent to lesion areas while in the aortic arch endothelial cells overlying intimal lesions were 15-LO(+). Subendothelial intimal cells which were characterized as RAM11(−), small, very basophilic and located in superficial intimal regions were also found to be 15-LO(+) in 12% of the animals (Fig. 9B). No consistent 15-LO staining was evident in deep-intimal RAM11(+) monocyte–macrophage foam cells. Positive 15-LO staining was also found in the adventitia associated with RAM11(−), small, very basophilic cells (Fig. 9B) in 55% of the animals and with cells of periadventitial lymph nodes in most animals. Medial cells and SMC did not stain with antibodies to 15-LO.

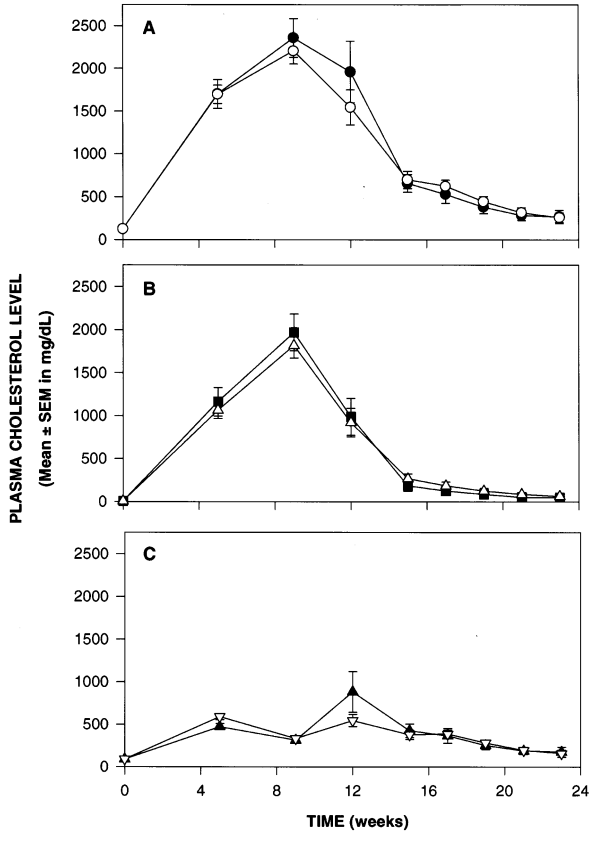

Fig. 4. Line plot of plasma total (Panel A), VLDL- (Panel B) and LDL-cholesterol (Panel C) concentrations over the course of the lesion regression study. Data are expressed as mean ± S.E.M. in mg/dl after treatment with 175 mg/kg PD146176, qd. Plasma total, VLDL- or LDL-cholesterol concentrations were not significantly different from the progression control at $P < 0.05$ over the course of the study. Filled symbols refer to the progression control while open symbols represent PD146176 (175 mg/kg, q.d.). Total cholesterol: ● and ○. VLDL-cholesterol: ■ and △. LDL-cholesterol: ▲ and ▽.

4. Discussion

Inhibition of 15-LO with PD146176 in the absence of changes in plasma cholesterol exposure and irrespective of whether the compound was administered before or after atherosclerotic lesion formation, can limit the monocyte–macrophage foam cell enrichment of atherosclerotic lesions and attenuate the development of both foam cell-rich lesions and more complex fibrous plaques. This conclusion is based on several findings of the present study, which can be outlined as follows: (1) plasma total and lipoprotein cholesterol exposure as measured by the area under the cholesterol-time curve associated with the drug treatment phase were similar in control and PD146176-treated animals in both the progression and regression studies. (2) In the progression study, monocyte–macrophage RAM11(+) cell area in the chronically injured iliac-femoral artery was reduced 71% by PD146176 despite comparable cross-sectional lesion areas. (3) In the regression study, the gross extent of thoracic aortic lesions was reduced 41% and both the size and macrophage content of complex fibrous plaque-like lesions in the iliac-femoral artery were decreased 34%. In addition to the observation that PD146176 can limit atherosclerotic lesion development, these findings suggest that 15-LO or 15-LO products may be involved in the recruitment, differentiation and lipid enrichment of monocyte–macrophages within the atherosclerotic lesion.

Plasma total and lipoprotein cholesterol exposure were comparable among groups in both the progression and regression studies. However, a consistent 2- to 4-fold increase in plasma triglyceride exposure was noted in both studies. Based on the work of Heek and Zilversmit who have shown that there is an inverse

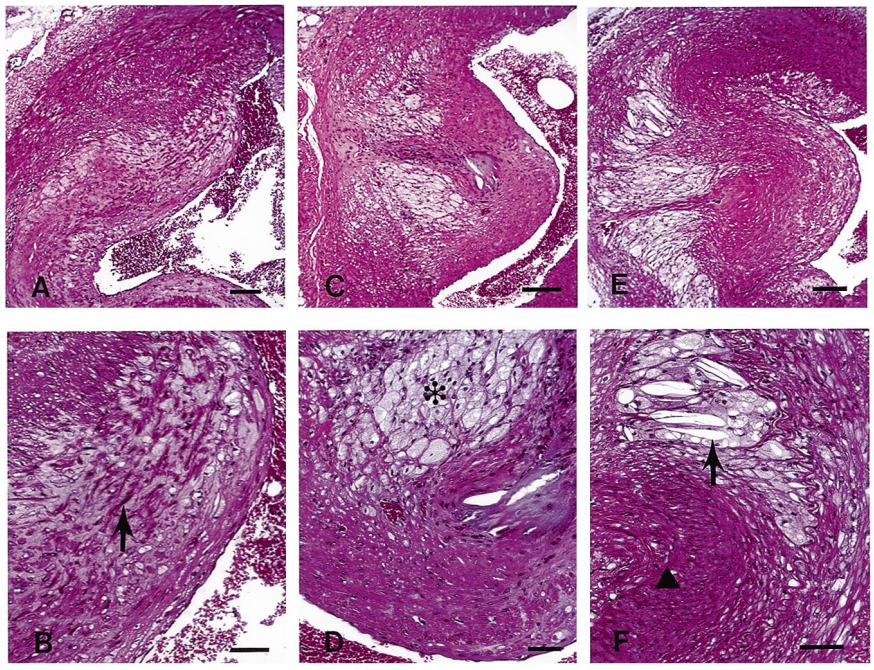

Fig. 5

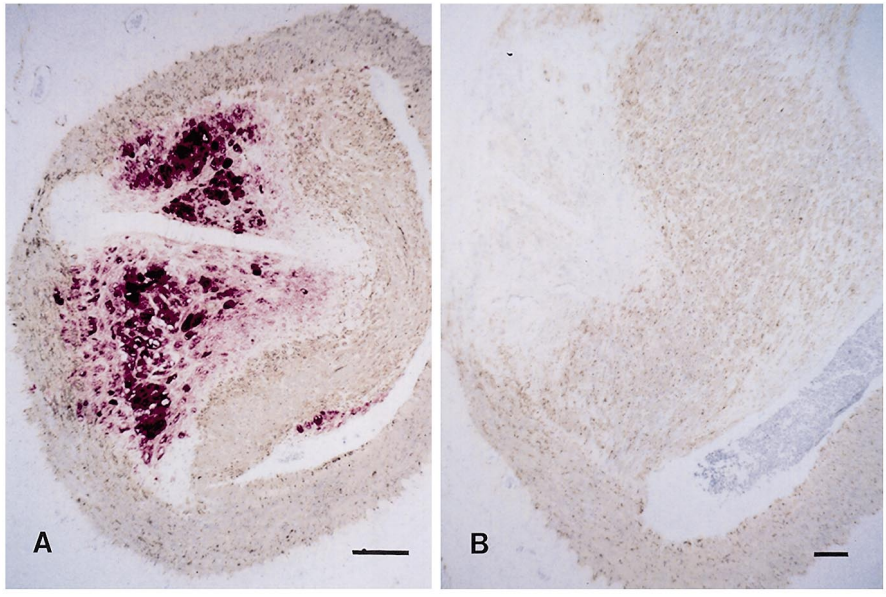

Fig. 6

Fig. 5. Photomicrographs of the general histologic appearance of the three major lesion types observed in the iliac-femoral artery. Panel A: fibromuscular lesion. Hematoxylin and eosin (H and E); × 100; bar = 100 μm. Panel B: higher magnification of Panel A denoting the abundant SMC (arrow) and matrix. H and E; × 250; bar = 50 μm. Panel C: fibrofoamy lesion. H and E; × 100; bar = 100 μm. Panel D: higher magnification of Panel C. Note the presence of monocyte–macrophage foam cells (asterisk) within this lesion type. H and E; × 250; bar = 50 μm. Panel E: fibrous plaque lesion. H and E; × 100; bar = 100 μm. Panel F: higher magnification of Panel E. The presence of a fibrous cap (arrowhead) and free cholesterol clefts (arrow) discriminate this lesion from the fibrofoamy lesion. H and E; × 250; bar = 50 μm.

Fig. 6. Photomicrographs of the relative monocyte–macrophage extents in control (Panel A) and PD146176-treated (175 mg/kg, b.i.d.) (Panel B) animals. The photomicrographs are representative of lesions with approximate mean lesion and macrophage area for each treatment group. Monocyte–macrophages are stained using RAM11 and appear red in both micrographs. Avidin–biotin-peroxidase staining procedure with Vector Red as chromogenic substrate. Smooth muscle cells are stained using HHF35 and appear brown in both micrographs. Avidin–biotin-peroxidase staining procedure with DAB as chromogenic substrate. × 100; bar = 100 μm.

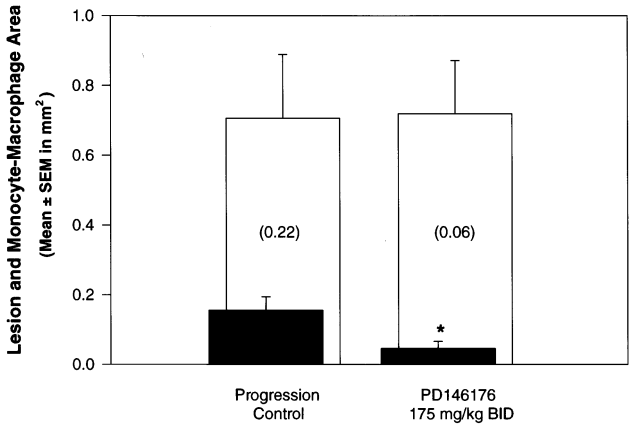

Fig. 7. Bar graph of the morphometric data for the iliac-femoral lesion in the progression study. Data are expressed as the mean ± S.E.M. RAM11(+) monocyte–macrophage area ■ and total lesion area □. Value in parenthesis represents the monocyte–macrophage/lesion ratio. *, denotes a significant difference in macrophage area from the progression control at $P < 0.05$.

relationship between plasma triglyceride levels and atherosclerotic lesion cholesterol enrichment [38], one might attribute the antiatherosclerotic activity of PD146176 in part to the hypertriglyceridemia. However, the major difference between the study by Heek and Zilversmit and the current investigation is that

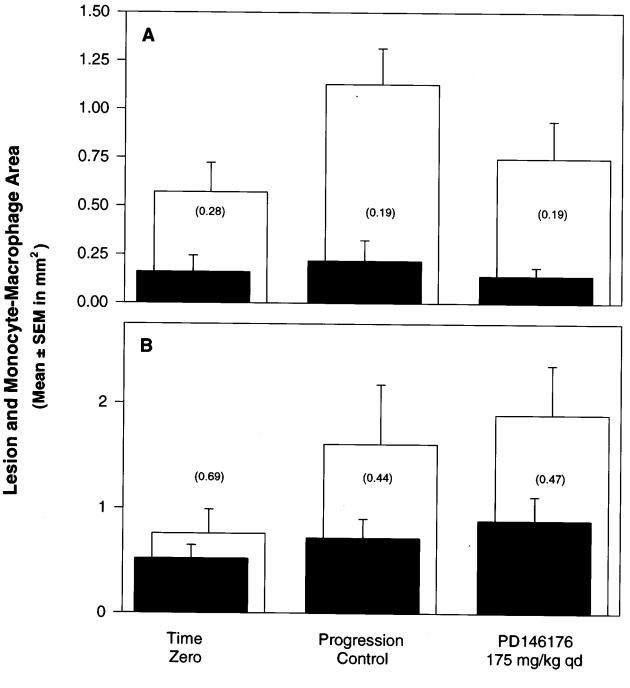

Fig. 8. Bar graph of the morphometric data for the iliac-femoral (Panel A) and aortic arch (Panel B) lesions in the regression study. Data are expressed as the mean ± S.E.M. RAM11(+) monocyte–macrophage area ■ and total lesion area □. Value in parenthesis represents the monocyte–macrophage/lesion ratio. No significant difference in monocyte–macrophage or lesion area were noted at $P < 0.05$; however, at $P < 0.10$ PD146176 significantly decreased lesion area.

plasma triglyceride levels were approximately 3-fold higher than in the current study. Based on the work of several investigators who have shown that triglyceride-rich VLDL and plasma chylomicrons promote foam cell formation [39], one might propose that the level of hypertriglyceridemia achieved in this study was proatherogenic. Despite the proatherogenic properties of triglyceride-rich lipoprotein particles, PD146176 decreased the cholesteryl ester content of the iliac-femoral artery and thoracic aortic lesions irrespective of whether the compound was administered coincident with lesion induction or after establishment of a fibrofoamy lesion. Associated with the reduction in vascular cholesteryl ester content was a decrease in monocyte–macrophage foam cell accumulation. These data suggest that PD146176 limits the monocyte–macrophage and lipid enrichment of atherosclerotic lesions not only in the absence of a change in plasma total and lipoprotein cholesterol exposure but also in the presence of a modest hypertriglyceridemia.

Although there was no change in plasma total or lipoprotein cholesterol exposure as determined by quantification of the area under the respective cholesterol-time curves, mean final plasma total and VLDL-cholesterol levels were reduced. In the progression study, plasma total cholesterol concentrations in the PD146176-treated animals were comparable to controls over the first 8 weeks; however, at necropsy plasma total and VLDL-cholesterol concentrations were reduced 47 and 66%, respectively. Reductions in plasma cholesterol levels could account for changes in lesion extent and lipid enrichment; however, we have reported that plasma cholesterol exposure is more predictive of the degree of atherosclerosis [40]. In both the progression and regression studies, plasma total cholesterol exposure was comparable among the groups. In addition, no change in mean plasma total and lipoprotein cholesterol levels were noted in the regression study; yet, PD146176 blunted the further progression of atherosclerotic lesions. Thus, one can conclude that the antiatherosclerotic activity of PD146176 appears to be mediated by a direct action of the compound on macrophage accumulation and not an indirect response to cholesterol lowering.

One mechanism for the observed antiatherosclerotic activity of PD146176 which is unrelated to any hypolipidemic activity may relate to inhibition of 15-LO mediated oxidative modification of insudant lipoproteins and therefore a decrease in proatherogenic species necessary for cellular lipid accumulation. Oxidative modification of plasma lipoproteins and then subsequent unregulated uptake by macrophages may be a mechanism for foam cell formation [1]. The products of 15-LO, i.e. lipid hydroperoxides, may initiate lipoprotein oxidation and therefore promote foam cell formation. Investigators have colocalized the 15-LO gene

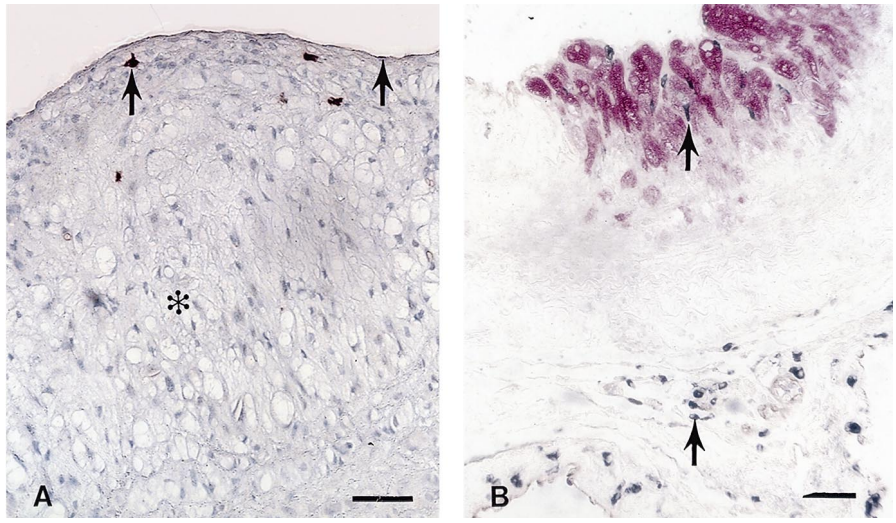

Fig. 9. Photomicrographs of the 15-LO staining patterns within the iliac-femoral artery. Panel A: note the focal 15-LO(+) endothelial cells and monocyte-like cells which are stained blue-black (arrow) while the foamy appearing monocyte–macrophages (*) are 15-LO(−). Panel B: note the 15-LO(+) monocytic cells located in superficial regions of the intima and adventitital fibroblasts which appear stained blue-black (arrow). RAM11(+) monocyte–macrophages are red as are 15-LO(−). Avidin–biotin-peroxidase staining procedure using Vector Red and BCIP/NBT (5-bromo-4-chloro-3-indolyl phosphate/nitro blue tetrazolium) as chromogenic substrate to generate the red and blue-black reaction products, respectively. × 100; bar = 100 μm.

[15,41], stereospecific products of the 15-LO enzyme [17], 15-LO mRNA and epitopes of oxidized LDL with macrophage-rich areas of atherosclerotic lesions [19]. Although the data are circumstantial, the published findings implicate 15-LO and/or 15-LO products in the disease process by presumably seeding the oxidation of lipoproteins retained in the vessel wall.

If 15-LO and/or 15-LO products are primarily involved in the initiation of lipoprotein oxidation, one might suspect that inhibitors of 15-LO would only prevent the development of atherosclerotic lesions when administered coincident with hypercholesterolemia. In addition to reducing the iliac-femoral monocyte–macrophage area in the progression study, PD146176 decreased the formation and macrophage enrichment of atherosclerotic lesions when administered to animals with pre-established lesions and after an extended period of hypercholesterolemia, i.e. 15 weeks, as noted in the regression study. One might suspect that the seeding reactions required for lipoprotein modification would have occurred during the 15-week lesion induction phase and further oxidative modification during the drug treatment phase may be of a nonenzymatic origin. Such an hypothesis is consistent with the work of Kuhn et al., who have shown that the ratio of *S*- to *R*-isomers of 13-hydroxy-9*Z*,11*E*-octadecadienoic acid (13-HODE) was 7:3 at 12 weeks of cholesterol feeding while at later time points the pattern of oxygenated products lacked chiral specificity for the enzyme produced *S*-enantiomer [15].

Inhibition of lipoprotein oxidation by the 15-lipoxygenase inhibitor, PD146176, is one explanation for the results of this study; however, the magnitude and types of lesion changes is inconsistent with the activity of general antioxidants. We have previously shown in a similar animal model of atherosclerosis that probucol, a lipid-lowering agent with antioxidant properties and systemically bioavailable, decreased the cholesteryl ester enrichment of the thoracic aorta but had no effect on the extent, cross-sectional area or monocyte–macrophage content of atherosclerotic lesions despite a 41% reduction in plasma cholesterol concentration [11]. In another study, combination of vitamins E and C reduced the cholesteryl ester content and extent of atherosclerosis in the thoracic aorta by 42–46% but like probucol had no effect on the more complex iliac-femoral lesion [11]. Other investigators have shown that combination of vitamins E and A can blunt thoracic aortic cholesteryl ester enrichment [42] while others have reported that vitamin E had no effect on the development of balloon injury-induced atherosclerotic lesions [43]. Another antioxidant, butylated hydroxytoluene (BHT), has been shown to decrease the extent of dietary cholesterol-induced thoracic aortic atherosclerosis [44]. The published data indicate that general antioxidants have some antiatherosclerotic activity; however, the variability of the results, the preferential effect on foam cell enriched lesions and the marginal antiatherosclerotic activity of probucol in the presence of plasma cholesterol lowering suggests that PD146176 may have a more direct effect on the biology of the vascular cells.

Consistent with the hypothesis that PD146176 may have a direct affect on monocyte–macrophage accumulation in the intima is the observation that 15-LO staining is associated with specific cell types within the

atherosclerotic lesion. Focal areas of endothelial cells, subendothelial, RAM11(−), small, very basophilic cells and adventitial fibroblasts stain positively for 15-LO while intimal or medial smooth muscle cells or deep-intimal macrophage staining is absent. The observed 15-LO staining pattern is similar to that of other investigators who evaluated 15-LO mRNA and antigen distribution [15,17,41] except that we did not observe the abundant intimal macrophage staining. The apparent differences in macrophage immunostaining pattern may relate to differences in antibody preparations. It is possible that the antibody used in the current investigation recognizes an epitope of 15-LO which is either masked or destroyed in areas of macrophage enrichment and this might account for the disparity. The rabbit model of atherosclerosis in which a chronic endothelial injury is combined with diet-induced hypercholesterolemia is another difference between the current and previous studies. However, a staining pattern similar to that noted here was seen in aortic arch lesions of rabbits fed the cholesterol/fat diet without chronic endothelial denudation (unpublished data, 1996). Despite the disparity, the most intriguing finding is the consistent subendothelial localization of 15-LO(+), RAM11(−), small basophilic cells and focal endothelial 15-LO(+) cells.

Direct inhibition of 15-LO by PD146176 within the vessel has not been shown; however, plasma drug concentrations of up to 214 ng/ml which approximates the K_i of 197 ng/ml and is one-half the IC_{50} against rabbit reticulocyte 15-LO have been achieved in both experiments. As noted above, 15-LO protein [17], mRNA [14–18] and stereospecific enzyme products [15,16] have been found in atherosclerotic lesions. Based on the pharmacokinetic data and the localization of 15-LO in the vessel, one can conclude that there is evidence to indicate that the antiatherosclerotic activity of PD146176 may be mediated through inhibition of 15-LO. Evidence supporting direct inhibition of 15-LO within the arterial wall as a mechanism for the observed antiatherosclerotic activity is difficult to obtain due to the nature of the oxidation process. For instance, it is presumed that the lipid hydroperoxides generated by the 15-LO reaction initiates a series of pro-oxidant events which modify vessel wall retained lipoproteins. Kuhn et al. [15] has observed that after protracted cholesterol feeding stereospecific products of 15-LO cannot be identified. The absence of chiral 15-LO products in organic extracts of atherosclerotic vessels taken after 12 and 23 weeks of cholesterol feeding is expected and would not provide any further evidence for the direct involvement of PD146176. In addition, we attempted to isolate tracheal epithelial cells from control and PD146176-treated animals as a potential ex vivo surrogate of in vivo 15-LO inhibitory activity. Tracheal epithelial cell 15-LO activity was unaffected in the treated animals (Welch, unpublished data, 1997). The lack of activity is not surprising given the observation that PD146176 appears to be a reversible inhibitor of 15-LO which can be washed out of cells following a 40 min incubation without drug. The data although circumstantial indicates that PD146176 through inhibition of 15-LO may limit the macrophage enrichment of atherosclerotic lesions; however, in vivo proof of direct inhibition of arterial 15-LO requires additional scientific investigation.

In contrast to our hypothesis that inhibition of 15-LO may be antiatherosclerotic, a recent study by Shen et al. [45] indicates that specific expression of 15-LO in monocyte–macrophages may be atherosclerosis-protective in hypercholesterolemic rabbits. Based on the histologic data noted above, minimal staining was seen in monocyte–macrophages of atherosclerotic lesions while endothelial cells stained consistently with antibodies to 15-LO. Further evidence which suggests that endothelial cell expression of 15-LO may be pro-atherogenic can be found in a recent abstract by Harat et al. [46]. Overexpression of 15-LO in the endothelium of mice lacking the LDL receptor promotes atherosclerotic lesion formation [46]. Although one cannot rule out the atheroprotective effect of specific monocyte expression of 15-LO in hypercholesterolemic transgenic rabbits, it would appear that inhibition of 15-LO is antiatherosclerotic in classical models of diet- and endothelial injury-induced atherosclerosis. One can speculate as to the reasons for the disparity but it is apparent that a major difference between the animal models relates to the cell type specific expression of 15-LO. One might conclude that hypercholesterolemia-induced endothelial expression of 15-LO stimulates a cascade of events which promotes monocyte–macrophage accumulation in the arterial wall while the artificial overexpression of 15-LO in monocytes may change the cell phenotype and limit atherosclerotic lesion development.

Based on the histologic data, one might speculate that 15-LO may be involved in the adhesion and diapedesis of monocytes into the intima and that inhibition of 15-LO would specifically prevent the accumulation of intimal monocyte–macrophages. This speculation is based upon the observations that adhesion molecules and 15-LO may have common regulatory cytokines and that both overexpression and products of the 15-LO enzyme can regulate adhesion molecules and monocyte migration. The adhesion molecule, VCAM-1, has been shown to be involved in monocyte adhesion to vascular endothelial cells [47] and to be regulated by IL-4 and IFN-γ [23] which are two cytokines shown to be potent regulators of monocyte 15-LO expression [48]. In addition, transient overexpression of 15-LO in endothelial cells has been shown to enhance TNF-induced VCAM-1 expression [24]. Sul-

tana et al. [49] have also shown that products of 15-LO i.e. 15(*S*)-hydroperoxy-5,8,11,13-eicosa-tetraenoic acid (15[*S*]-HPETE), at nM concentrations not only increase adhesion molecule expression but also increase transendothelial migration of HL-60 monocytic cells. Given the colocalization of 15-LO staining on endothelial cells and subendothelial 15-LO(+), RAM11(−), small basophilic cells, the fact that IL-4 and IFN-γ both stimulate VCAM-1 and 15-LO expression, the recent observation that 15-LO products increase monocyte adhesion and migration and the presence of plasma drug concentrations sufficient to inhibit 15-LO, one might propose that inhibition of 15-LO by PD146176 reduced a common regulator of adhesion and immune/inflammatory reactions associated with atherosclerosis.

Acknowledgements

The authors would like to express their appreciation to Drs Bradley Tait and Bharat K. Trivedi and Norman Colbry for their efforts in preparing the large quantities of PD146176 needed to perform the study. We would also like to acknowledge Daniel Wilson and Jack Barbour for maintenance of the rabbit colony during the course of the study.

References

[1] Steinberg D, Parthasarathy S, Carew TE, Khoo JC, Witztum JL. Modifications of low density lipoprotein that increases its atherogenicity. New Engl J Med 1989;320:915.
[2] Smith EB, Evans PH, Pownham MD. Lipid in the aortic intima: the correlation of morphological and chemical characteristics. J Atheroscler Res 1967;7:171.
[3] Guyton JR, Bocan TMA, Schifani TA. A quantitative analysis of perifibrous lipid and its association with elastin in nonatherosclerotic human aorta. Arterioscler Res 1985;5:644.
[4] Rajavashisth TB, Andalibi A, Territo MC, Berliner JA, Navab M, Fogelman AM, Lusis AJ. Induction of endothelial cell expression of granulocyte and macrophage colony-stimulating factors by modified low-density lipoproteins. Nature 1990;344:254.
[5] Kume N, Cybulsky MI, Gimbrone MA Jr. Lysophosphatidylcholine, a component of atherogenic lipoproteins, induces mononuclear leukocyte adhesion molecules in cultured human and rabbit arterial endothelial cells. J Clin Invest 1992;90:1138.
[6] Daugherty A, Zweifel BS, Schonfeld G. Probucol attenuates the development of aortic atherosclerosis in cholesterol-fed rabbits. Br J Pharmacol 1989;98:612.
[7] Tawara K, Ishihara M, Ogawa H, Tomikawa M. Effect of probucol, pantethine and their combinations on serum lipoprotein metabolism and on the incidence of atheromatous lesions in the rabbit. Jpn J Pharmacol 1986;41:211.
[8] Carew TE, Schwenke DC, Steinberg D. Antiatherogenic effect of probucol unrelated to ist hypocholesterolemic effect: evidence that antioxidants in vivo can selectively inhibit low density lipoprotein degradation in macrophage-rich fatty streaks and slow the progression of atherosclerosis in Watanabe heritable hyperlipidemic rabbit. Proc Natl Acad Sci USA 1987;84:7725.
[9] Daugherty A, Zweifel BS, Schonfeld G. The effects of probucol on the progression of atherosclerosis in mature Watanabe heritable hyperlipidemic rabbits. Br J Pharmacol 1991;103:1013.
[10] Kita T, Nagano Y, Yokode M, Ishii K, Kume N, Ooshima A, Yoshia H, Kawai C. Probucol prevents the progression of atherosclerosis in Watanabe heritable hyperlipidemic rabbit, an animal model for familial hypercholesterolemia. Proc Natl Acad Sci USA 1987;84:5928.
[11] Bocan TMA, Bak Mueller S, Quenby Brown E, Uhlendorf PD, Mazur MJ, Newton RS. Antiatherosclerotic effects of antioxidants are lesion-specific when evaluated in hypercholesterolemic New Zealand white rabbits. Exp Mol Pathol 1992;57:70.
[12] Brattsand R. Actions of vitamins A and E and some nicotinic acid derivatives on plasma lipids and on lipid infiltration of aorta in cholesterol-fed rabbits. Atherosclerosis 1975;22:47.
[13] Bjorkhem I, Henriksson-Freyschuss A, Breuer O, Diczfalusy U, Berglund L, Henriksson P. The antioxidant butylated hydroxytoluene protects against atherosclerosis. Arterioscler Thromb 1991;11:15.
[14] Yla-Herttuala S, Rosenfeld ME, Parthasarathy S, Glass CK, Sigal E, Witztum JL, Steinberg D. Colocalization of 15-lipoxygenase mRNA and protein with epitopes of oxidized low density lipoprotein in macrophage-rich areas of atherosclerotic lesions. Proc Natl Acad Sci USA 1990;87:6959.
[15] Kuhn H, Belkner J, Zaiss S, Fahrenklemper T, Wohlfeil S. Involvement of 15-lipoxygenase in early stages of atherogenesis. J Exp Med 1994;179:1903.
[16] Folcik VA, Nivar-Aristy RA, Krajewski LP, Cathcart MK. Lipoxygenase contributes to the oxidation of lipids in human atherosclerotic plaques. J Clin Invest 1995;96:504.
[17] Hiltunen T, Luoma J, Nikkari T, Yla-Herttuala S. Induction of 15-lipoxygenase mRNA and protein in early atherosclerotic lesions. Circulation 1995;92:3297.
[18] Yla-Herttuala S, Rosenfeld ME, Parthasarathy S, Sigal E, Sarkioja T, Witztum JL, Steinberg D. Gene expression in macrophage-rich human atherosclerotic lesions. 15-Lipoxygenase and acetyl low density lipoprotein receptor messenger RNA colocalize with oxidation specific lipid–protein adducts. J Clin Invest 1991;87:1146.
[19] Rankin SM, Parthasarathy S, Steinberg D. Evidence for a dominant role of lipoxygenase(s) in the oxidation of LDL by mouse peritoneal macrophages. J Lipid Res 1991;32:449.
[20] Sendobry SM, Cornicelli JA, Welch K, Bocan T, Tait B, Trivedi BK, Colbry N, Dyer RD, Feinmark SJ, Daugherty A. Attenuation of diet-induced atherosclerosis in rabbits with a highly selective 15-lipoxygenase inhibitor lacking significant antioxidant properties. Br J Pharmacol 1997;120:1199.
[21] Khan BV, Parthasarathy S, Alexander RW, Medford RM. Modified low density lipoprotein and its constituents augment cytokine-activated vascular cell adhesion molecule-1 gene expression in human vascular endothelial cells. J Clin Invest 1995;95:1262.
[22] Couffinhal T, Duplaa C, Moreau C, Lamaziere JM, Bonnet J. Regulation of vascular cell adhesion molecule-1 and intercellular adhesion molecule-1 in human vascular smooth muscle cells. Circ Res 1994;74:225.
[23] Li H, Cybulsky MI, Gimbrone MA Jr., Libby P. Inducible expression of vascular cell adhesion molecule-1 by vascular smooth muscle cells in vitro and within rabbit atheroma. Am J Pathol 1993;143:1551.
[24] Wolle J, Welch KA, Devall LJ, Cornicelli JA, Saxena U. Transient overexpression of human 15-lipoxygenase in aortic endothelial cells enhances tumor necrosis factor-induced vascular cell adhesion molecule-1 gene expression. Biochem Biophys Res Comm 1996;220:310.
[25] Cushing SD, Berliner JA, Valente AJ, Territo MC, Navab M, Parhami F, Gerrity R, Schwartz CJ, Fogelman AM. Minimally

modified LDL induces monocyte chemotactic protein 1 in human endothelial and smooth muscle cells. Proc Natl Acad Sci USA 1990;87:5134.
[26] Young TE, Scott PH. Indolothiopyrylium compounds. I. Benz[b]indolo[2,3-d]thiopyrylium Perchlorates. A novel heteroaromatic ring system. J Org Chem 1965;30:3613.
[27] Allain CC, Poon LS, Chan CSG, Richmond W, Fu PC. Enzymatic determination of total serum cholesterol. Clin Chem 1974;20:470.
[28] Bucolo G, David H. Quantitative determination of serum triglycerides by the use of enzymes. Clin Chem 1973;19:476.
[29] Kieft KA, Bocan TMA, Krause BR. Rapid on-line determination of cholesterol distribution among plasma lipoproteins after high-performance gel filtration chromatography. J Lipid Res 1991;32:859.
[30] Folch J, Lees M, Sloane-Stanley GH. A simple method for the isolation and purification of total lipids from animal tissue. J Biol Chem 1957;226:497.
[31] Christie WW. Rapid separation and quantification of lipid classes by high performance liquid chromatography and mass (light-scattering) detection. J Lipid Res 1985;26:507.
[32] Thompson SW. Selected Histochemical and Histopathological Methods. Springfield, IL: Charles C. Thomas Publishing, 1966:1639.
[33] Tsukada T, Rosenfeld M, Ross R, Gown AM. Immunocytochemical analysis of cellular components in atherosclerotic lesions. Use of monoclonal antibodies with the Watanabe and fat-fed rabbit. Arteriosclerosis 1986;6:601.
[34] Gown AM, Vogel AM, Gordon D, Lu PL. A smooth muscle-specific monoclonal antibody recognizes smooth muscle actin isozymes. J Cell Biol 1985;100:807.
[35] Bocan TMA, Mazur MJ, BakMueller S, QuenbyBrown E, Sliskovic DR, O'Brien PM, Creswell MW, Lee H, Uhlendorf PD, Roth BD, Newton RS. Antiatherosclerotic activity of inhibitors of 3-hydroxy-3-methylglutaryl coenzyme A reductase in cholesterol-fed rabbits: a biochemical and morphological evaluation. Atherosclerosis 1994;111:127.
[36] Shanks ME, Gambill R. Calculus Analytic Geometry/Elementary Functions. New York: Holt, Rinehart and Winston, 1973:748.
[37] Ott L. An Introduction to Statistical Methods and Data Analysis. Massachusetts: Duxbury Press, 1977:730.
[38] Van Heek M, Zilversmit DB. Evidence for an inverse relation between plasma triglyceride and aortic cholesterol in the coconut oil/cholesterol-fed rabbit. Atherosclerosis 1988;71:185.
[39] Bradley WA, Gianturco SH. Triglyceride-rich lipoproteins and atherosclerosis: pathophysiological considerations. J Int Med 1994;236:33.
[40] Bocan TMA, Bak Mueller S, Mazur MJ, Uhlendorf PD, Quenby Brown E, Kieft K. The relationship between the degree of dietary-induced hypercholesterolemia in the rabbit and atherosclerotic lesion formation. Atherosclerosis 1993;102:9.
[41] Yla-Herttuala S. Gene expression in atherosclerotic lesions. Herz 1992;17:270.
[42] Brattsand R. Actions of vitamins A and E and some nicotinic acic derivatives on plasma lipids and on lipid infiltration of aorta in cholesterol-fed rabbits. Atherosclerosis 1975;22:47.
[43] Godfried SL, Combs GF, Saroka JM, Dillingham LA. Potentiation of atherosclerotic lesions in rabbits by a high dietary level of vitamin E. Br J Nutr 1989;61:607.
[44] Bjorkhem I, Henriksson-Freyschuss A, Breuer O, Diczfalusy U, Berglund L, Henriksson P. The antioxidant butylated hydroxytoluene protects agains atherosclerosis. Arterioscler Thromb 1991;11:15.
[45] Shen J, Hederick E, Cornhill JF, Zsigmond E, Kim HS, Kuhn H, Guevara NV, Chan L. Macrophage-mediated 15-lipoxygenase expression protects against atherosclerosis development. J Clin Invest 1996;98:2201.
[46] Harats D, Kurihara H, Levkovitz H, Sigal E. 15-lipoxygenase overexpression induces atherosclerosis in LDL deficient mice. Proc Eur Atheroscler Soc 1996;66:26.
[47] Cybulsky MI, Gimbrone MA. Endothelial expression of a mononuclear leukocyte adhesion molecule during atherogenesis. Science 1991;252:788.
[48] Conrad DJ, Kuhn H, Mulkins M, Highland E, Sigal E. Specific inflammatory cytokines regulate the expression of human monocyte 15-lipoxygenase. Proc Natl Acad Sci USA 1992;89:217.
[49] Sultana C, Shen Y, Rattan V, Kalra VJ. Lipoxygenase metabolites induced expression of adhesion molecules and transendothelial migration of monocyte-like HL-60 cells is linked to protein kinase C activation. J Cell Physiol 1996;167:477.